

# Power transformer protection using *S*-transform with complex window and pattern recognition approach

S.R. Samantaray, B.K. Panigrahi, P.K. Dash and G. Panda

**Abstract:** A new approach for power transformer protection using *S*-transform with complex window to distinguish between inrush current and internal fault is presented. The *S*-transform with complex window is used to extract patterns of transient current samples during inrush and faults. *S*-transform is a very powerful tool for non-stationary signal analysis giving the information of transient currents both in time and in frequency domains. The spectral energy is calculated for inrush and internal faults and an energy index is found out to distinguish between inrush magnetising current and internal faults. The simulation results and the results obtained using real-time data from a transformer in the laboratory environment indicate the robustness of the proposed technique.

## 1 Introduction

Power transformers play a vital role in any electric power system network. So it is very important to avoid any mal-operation and false tripping by providing required relaying system. Protection of large power transformers is a very challenging job in power system relaying. The phenomenon of inrush current in the power transformers has been well known for many years and is an important aspect of harmonic restraint differential relay. The inrush current contains a large second harmonic component in comparison to an internal fault. Sometimes, the second harmonic may be generated in the case of internal faults in power transformer also. This may be due to current transformer (CT) saturation and distributive capacitance in long transmission line to which the power transformer is connected. In certain cases, the magnitude of second harmonic in an internal fault current can be close to or greater than that present in the magnetising inrush current. Moreover, the second harmonic components in the magnetising inrush current tend to be relatively small in modern power transformer because of design improvements. Thus, the commonly employed conventional differential protection based on second harmonic restraint will face difficulty in distinguishing inrush current and internal faults. Thus, an improved technique of protection is required to discriminate between inrush current and internal faults.

As both inrush current and internal faults are non-stationary signals, the most important requirement is to extract features from the signal. For feature extraction or pattern recognition from non-stationary signal short time Fourier transform (STFT), discrete wavelet transform (DWT) has been used extensively. In the case of DWT [1, 2, 9, 10], the variations of the detailed coefficients are

obtained to distinguish between magnetising inrush and fault. The wavelet transform specifically decomposes a signal from high frequency to low frequency bands through an iterative procedure, and this procedure performs very well for high-frequency transients but not so well for low-frequency components including second-, third- and fifth-harmonic components of current present in the magnetising inrush or faults. Consequently, the wavelet decomposition coefficients in a frequency band reflect the overall effect of all signal components in the frequency band, rather than the specific fundamental and harmonic ones. Also the frequency properties of the decomposition filter bands are not ideal and suffer leakage effects where the signal frequency is closer to the edge of a frequency band. Therefore a more suitable signal processing technique is considered in this paper for recognising the current signal patterns in a transformer.

The *S*-transform is an invertible time–frequency spectral localisation technique [3–6] that combines elements of wavelet transform and STFT. The *S*-transform uses an analysis window whose width is decreasing with frequency providing a frequency-dependent resolution. *S*-transform is a continuous wavelet transform with a phase correction. It produces a constant relative bandwidth analysis like wavelets, although maintains a direct link with Fourier spectrum. The *S*-transform has an advantage in that it provides multiresolution analysis while retaining the absolute phase of each frequency. This has led to its application for detection and interpretation of non-stationary signals. Further, the *S*-transform provides frequency contours which clearly localises the signals at a higher noise level [7]. In this paper, a new pattern recognition approach using *S*-transform with complex window [8] is presented to distinguish between inrush and fault currents. As *S*-transform is obtained by multiplying the real window with Fourier sinusoid and Fourier sinusoid has time-invariant frequency, *S*-transform is unsuitable for resolving waveforms whose frequency changes with time. This problem can be overcome by using complex Gaussian window with a user-designed complex phase function. The phase function modulates the frequency of the Fourier sinusoid to give better time–frequency localisation of the time series. That means if the time series contains a specific sinusoidal waveform that is expected at all scales, then the complex Gaussian window

© The Institution of Engineering and Technology 2007

doi:10.1049/iet-gtd:20060206

Paper first received 28th April 2005 and in revised form 25th August 2006

S.R. Samantaray and G. Panda are with the National Institute of Technology, Rourkela, India

B.K. Panigrahi is with the Indian Institute of Technology, New Delhi, India

P.K. Dash is with the Centre for Research in Electrical, Electronics and Computer Engineering, Bhubaneswar, India

E-mail: pkdash\_india@yahoo.com

can give better time–frequency resolution of event signatures than the un-modulated, real-valued Gaussian window of the original signal.

When a fault occurs on the secondary side of a transformer, the transient current is captured by the respective CTs at primary and secondary sides of the transformer. Also inrush current is captured in the same way. After the signal is retrieved,  $S$ -transform is used to process the signal samples to provide the relevant features for detection and recognition. The spectral energy of inrush current and fault current at different contour levels are computed from the  $S$ -transform output matrix. From the spectral energy, an energy index is calculated which discriminates between inrush and fault current and the relay restrains or operates accordingly. Also time–frequency contours in both fault and inrush are presented to distinguish both the events.

## 2 S-transform with complex window

The generalised  $S$ -transform is defined as

$$S(\tau, f, p) = \int_{-\infty}^{\infty} h(t) \{w(\tau - t, f, p) \times \exp(-2\pi ift)\} dt \quad (1)$$

where  $w$  is the window function of the  $S$ -transform and  $p$  denotes the set of parameters that determines the shape and property of the window function,  $w$ .

The alternative expression of (1) using Fourier transform can be given as

$$\int S(\tau, f, p) = \int_{-\infty}^{\infty} H(\alpha + f) W(\alpha, f, p) \times \exp(+2\pi i\alpha\tau) d\alpha \quad (2)$$

where

$$H(f) = \int_{-\infty}^{\infty} h(t) \exp(-2\pi ift) dt \quad (3)$$

$$W(\alpha, f, p) = \int_{-\infty}^{\infty} w(t, f, p) \exp(-2\pi i\alpha t) dt \quad (4)$$

The variables  $\alpha$  and  $f$  in the above expression have the same units.

For  $S$ -transform to converge to Fourier transform  $H(f)$

$$\int_{-\infty}^{\infty} S(\tau, f, p) d\tau = H(f) \quad (5)$$

For  $w$  to be the window of  $S$ -transform, the following condition must be satisfied

$$w(\tau - t, f, p) \exp(-2\pi ift) = A(\tau - t, f, p) \times \exp\{-2\pi i\phi(\tau - t, f, p)\} \quad (6)$$

where  $A$  and  $\phi$  are the amplitude and phase of  $w$ . If both sides are multiplied by Fourier sinusoids,  $w$  becomes

$$w(\tau - t, f, p) \exp(-2\pi ift) = A(\tau - t, f, p) \exp\{-2\pi i[ft + \phi(\tau - t, f, p)]\} \quad (7)$$

As the amplitude  $A$  and phase angle  $\phi$  of the  $S$ -transform output are known, the instantaneous frequency  $F$  can be defined as the time derivative of the total phase

$$F = f + \frac{\partial}{\partial t} \phi(\tau - t, f, p) \quad (8)$$

The  $S$ -transform gives the best localised spectrum when the

analysing function matches with the shape of the time series of the signal. The analysing function is defined by the multiplication of the Fourier sinusoid with the Gaussian window with phase modulation through an appropriate complex factor and normalisation. This gives to complex Gaussian window  $w_{cg}$  as

$$w_{cg}(\tau - t, f, \sigma) = \begin{cases} p \exp\left[-\frac{f^2(\tau - t)^2}{2}\right] \exp\left\{\begin{array}{l} -2\pi if(\tau - t) \\ +2\pi i \text{sign}(f) \sigma \\ \log[\sigma + |f|(\tau - t)] \end{array}\right\}, & t \leq \tau + \frac{\sigma}{|f|} \\ 0, & t \geq \tau + \frac{\sigma}{|f|} \end{cases} \quad (9)$$

The pre-factor  $p$  is defined as

$$p^{-1} = \int_{-\sigma/|f|}^{\infty} \exp\left\{-\frac{f^2\tau^2}{2} - 2\pi if\tau + 2\pi i \text{sign}(f) \times \sigma \log[\sigma + |f|\tau]\right\} d\tau \quad (10)$$

where the positive parameter  $\sigma$  controls the degree of phase modulation. When  $w_{cg} \neq 0$ , the instantaneous frequency becomes

$$F = \frac{\sigma f}{\sigma + |f|(\tau - t)} \quad (11)$$

The discrete  $S$ -transform is obtained by sampling (2) in the frequency domain and is given by

$$S_{cg} = \left[ jT, \frac{n}{MT}, p \right] = \sum_{m=-M/2}^{M/2-1} H\left[\frac{n+m}{MT}\right] \times W_{cg}\left[\frac{m}{MT}, \frac{n}{MT}, p\right] \times \exp\left[\frac{+2\pi imj}{M}\right] \quad (12)$$

where  $T$  is the sampling interval,  $M$  the number of sample points and  $j$  the discrete time index.  $m$  and  $n$  are discrete frequency indices.

The discrete window function is obtained by

$$W_{cg}\left[\frac{m}{MT}, \frac{n}{NT}, \sigma\right] = p \sum_{k=\max(-\sigma M/|n|, -M/2)}^{M/2-1} \exp\left[\frac{-n^2}{2M^2} - \frac{2\pi ink}{M}\right] \times \exp\left\{-2\pi i\left[\frac{nk}{M} - \sigma \text{sign}(n)\right]\right\} \times \log\left(\sigma + \frac{|n|k}{M}\right) \quad (13)$$

where  $p$  is defined as

$$p^{-1} = p \sum_{k=\max(-\sigma M/|n|, -M/2)}^{M/2-1} \exp\left[\frac{-n^2 k^2}{2M^2}\right] \times \exp\left\{-2\pi i\left[\frac{nk}{M} - \sigma \text{sign}(n)\right] \times \log\left(\sigma + \frac{|n|k}{M}\right)\right\} \quad (14)$$

and  $k$  is the discrete time index.

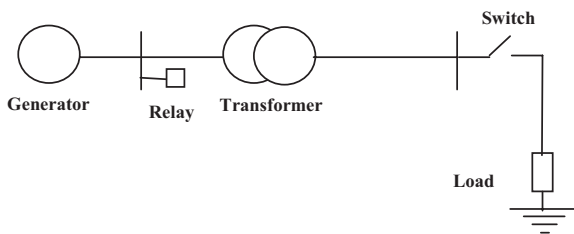


Fig. 1 System model

### 3 System studied

The simulation study has been done on the system comprising a 2000 MVA generator and 1000 MVA with 500 kV/220 kV transformer shown in Fig. 1. The generator  $X/R$  ratio is 10. The primary winding voltage,  $R$  (pu) and  $L$  (pu) are 500 kV, 0.003 and 0.09, respectively, and secondary winding voltage,  $R$  (pu) and  $L$  (pu) are 220 kV, 0.003 and 0.09, respectively. Also simulation tests are done on 100 MVA capacity transformer with other parameters remaining the same. The winding configuration such as Y-Y, Y-D, D-Y and D-D are taken into consideration for extensive study. The study has been made for both inrush current and different internal faults with and without load. Faults are created for winding-to-ground, winding-to-winding with and without load. The sampling rate is chosen 1.0 kHz at 50 Hz frequency. A cycle contains 20 samples. One cycle data of inrush and fault have been processed through  $S$ -transform to give the spectral energy at different contour levels. The simulation model is developed using Matlab–Simulink software modules. For studying the performance of the proposed approach under noisy conditions, random noise with SNR up to 20 dB has been added to the differential current signal. The load taken here is 100 MW and 80 MVAR.

Also real-time tests (experimental) have been conducted for a single-phase transformer of 5 kVA capacity with 400 V/230 V in the laboratory. The winding configuration is Y–Y for the experimental set-up. The inrush current and internal faults like winding-to-winding and winding-to-ground for different turn positions are measured by using a power scope.

## 4 Results and discussion

### 4.1 Differential protection based on second harmonic restraint

The differential protection based on second harmonic restraint using adaptive linear combiner (ADALINE) [13] is tested. The results of differential protection based on second harmonic restraint are given in Fig. 2. A factor of 6 is multiplied to the actual amplitude of the second harmonic component present in the current waveform to produce the restraint signal. The operating signal is the magnitude of the fundamental component. As seen from the Fig. 2a, the tripping signal for inrush and fault based on second harmonic restraint using ADALINE are well separated and a threshold can be set for the tripping signal above which relay restrains (inrush) and below which relay operates (fault). This is possible when the second harmonic magnitude compared with fundamental exceeds 20% and the fault current has a lower second harmonic component compared with the fundamental component. But when the second harmonic component is nearly 10% in both the

cases, the tripping signal for internal fault and inrush current overlap each other and no threshold can be set for the tripping signal as shown in Fig. 2b. Thus, the second harmonic restraint fails in such cases having low second harmonic component compared with the fundamental.

The above problem is solved by the proposed method, which discriminates the inrush current and internal fault even if the second harmonic component is same in both inrush and internal fault with the existing operating conditions and configurations. In this case, the proposed energy index is 2.57 for inrush current and 3.89 for internal faults, which are well separated with the set threshold. The generated  $S$ -contours for inrush and internal faults are given in Figs. 2c and d, respectively. The  $S$ -contours with contour level 1 for inrush and internal fault are given in Figs. 2e and f, respectively. The above study is made on synthesising the inrush and fault current and processing the respective signals through ADALINE and  $S$ -transform. After confirming the results on synthesised data, the corresponding signals for simulation models and experimental set-up are tested and the results are given in the following sections.

### 4.2 Feature extraction using $S$ -transform

Data for inrush current and internal faults are generated from the simulation model given in Fig. 1. The  $S$ -transform of the corresponding data is computed. The frequency contours ( $S$ -contours) and the spectral energy (energy) of  $S$ -transform of inrush current and fault signals are calculated for one cycle data from the inception of inrush and fault conditions. The frequency contours (levels 1–9) are shown in Figs. 3a–h with frequency. But the frequency contours for contour level 1 is obtained as shown in Figs. 4a–h for simulation data. It is clear from the frequency contour ( $S$ -contour) with contour levels 1–9 that in case of inrush current, the contours are present only during positive peaks of the current waveform compared with various fault conditions. For faults occurring on the transformer, the frequency contours are found with positive and negative sections of the fault current waveform. However,  $S$ -transform output contour level 1 for inrush current shows that the frequency contour is concentric around second harmonic frequency, and in the case of faults, the frequency contours are around fundamental frequency. Similarly, the data retrieved from real-time transformer tests in the laboratory are processed through  $S$ -transform to yield the frequency contours for both inrush current and internal faults. The frequency contours for real-time generated data are as shown in Figs. 5a–c with contour levels 1–9. Figs. 6a–c depict frequency contours at contour level 1 only for real-time data. From the figures, it is clearly seen that the inrush current having different frequency contours exhibits interrupted patterns in comparison to internal fault current showing regular patterns.

Tables 1 and 2 depict the spectral energy content of inrush current and internal faults for various conditions. It is clearly seen that the spectral energy content of inrush currents are much less when compared with the spectral energy content of internal faults for  $S$ -contours with contour levels 1–9. But the spectral energy content of inrush current is more than that of internal faults for  $S$ -contours with contour level-1 only. The energy calculations lead to the energy index which discriminates inrush current from internal faults.

### 4.3 Energy index to distinguish inrush current from faults

From the above results, energy index is found out to distinguish inrush current from internal faults. The energy

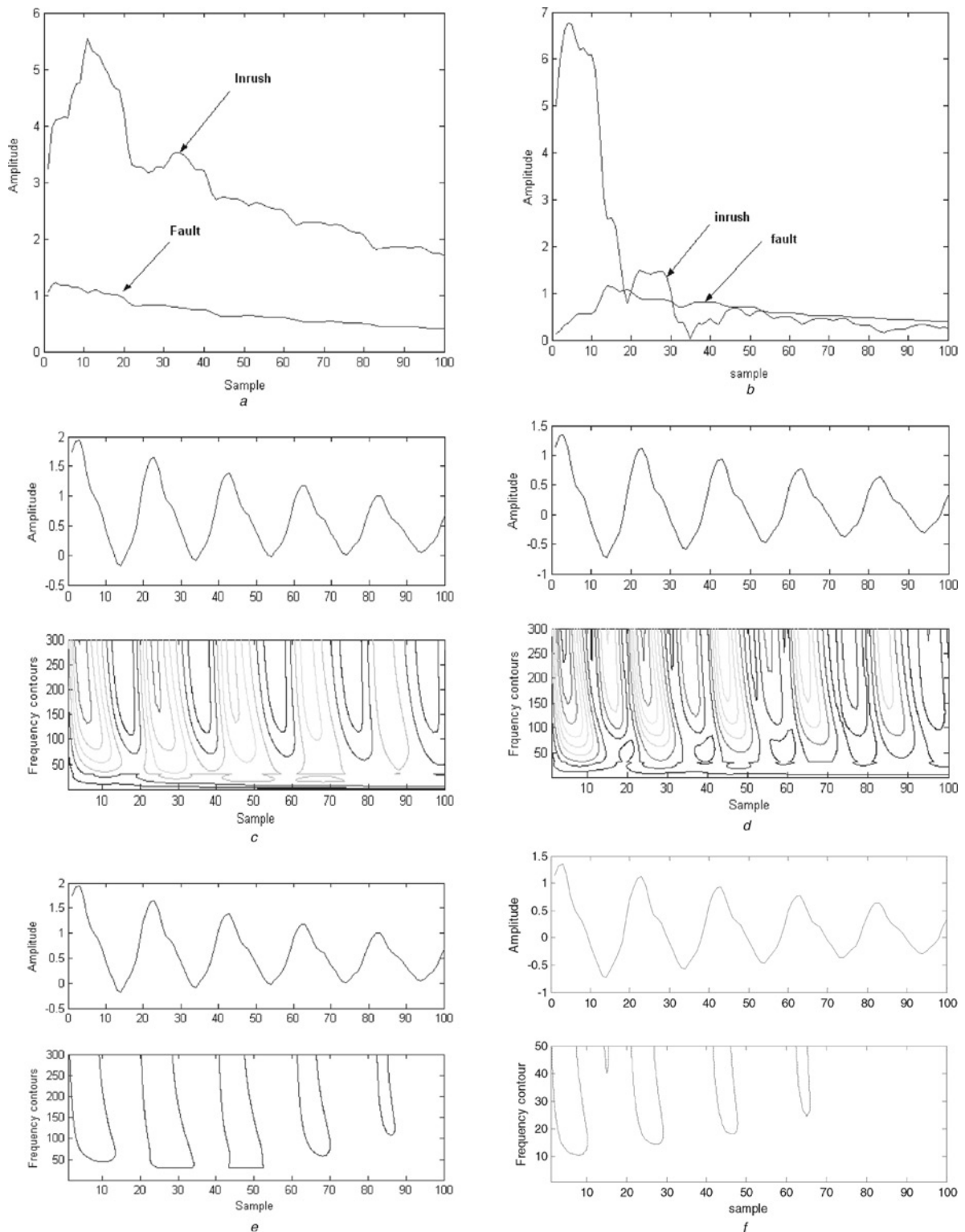


**Fig. 2** Results of differential protection based on the second harmonic restraint and proposed *S*-transform based technique for synthesised data

*a* Tripping signals obtained from ADALINE when the second harmonic component is 60 and 10% in inrush current and fault, respectively

*b* Tripping signals obtained from ADALINE when the second harmonic component is 10% in both inrush current and fault, respectively

*c* *S*-contours for inrush current

*d* *S*-contours for internal fault

*e* *S*-contours for inrush current at contour level 1

*f* *S*-contours for internal fault at contour level 1

index is given as

$$\text{Energy index} = \frac{\text{Energy of } S\text{-contours with contour level-1 to contour level-9}}{\text{Energy of } S\text{-contours with contour level-1}} \quad (15)$$

The devised index has been derived from the ratio of energy of *S*-contours from levels 1–9 to energy of *S*-contours at level 1, which clearly indicates that the ratio of energy content of all harmonic components to the energy of the fundamental or second harmonic depends on the kind of events under analysis, inrush or fault. The energy index is 1.09 (minimum) and 1.22 (maximum) for inrush current

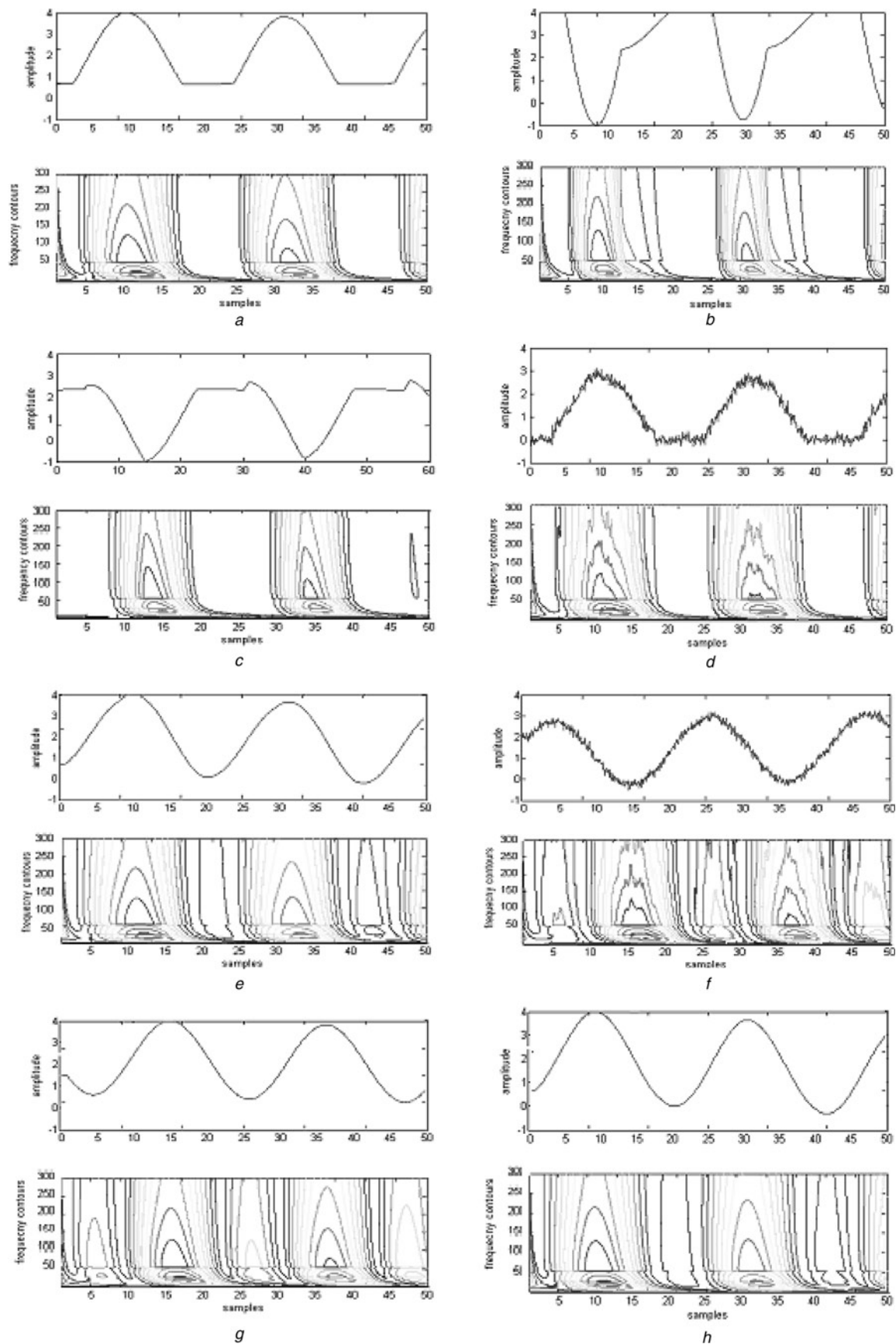


**Fig. 3** Frequency contours for simulation data

- a* *S*-contours for inrush current of a-phase
- b* *S*-contours for inrush current of b-phase
- c* *S*-contours for inrush current of c-phase
- d* *S*-contours for inrush current of a-phase with SNR 20 dB
- e* *S*-contours for winding to ground fault of a-phase
- f* *S*-contours for winding to ground fault of c-phase with SNR 20 dB
- g* *S*-contours for winding to ground fault of b-phase with load
- h* *S*-contours for winding to winding fault of a-c with load (a-phase)

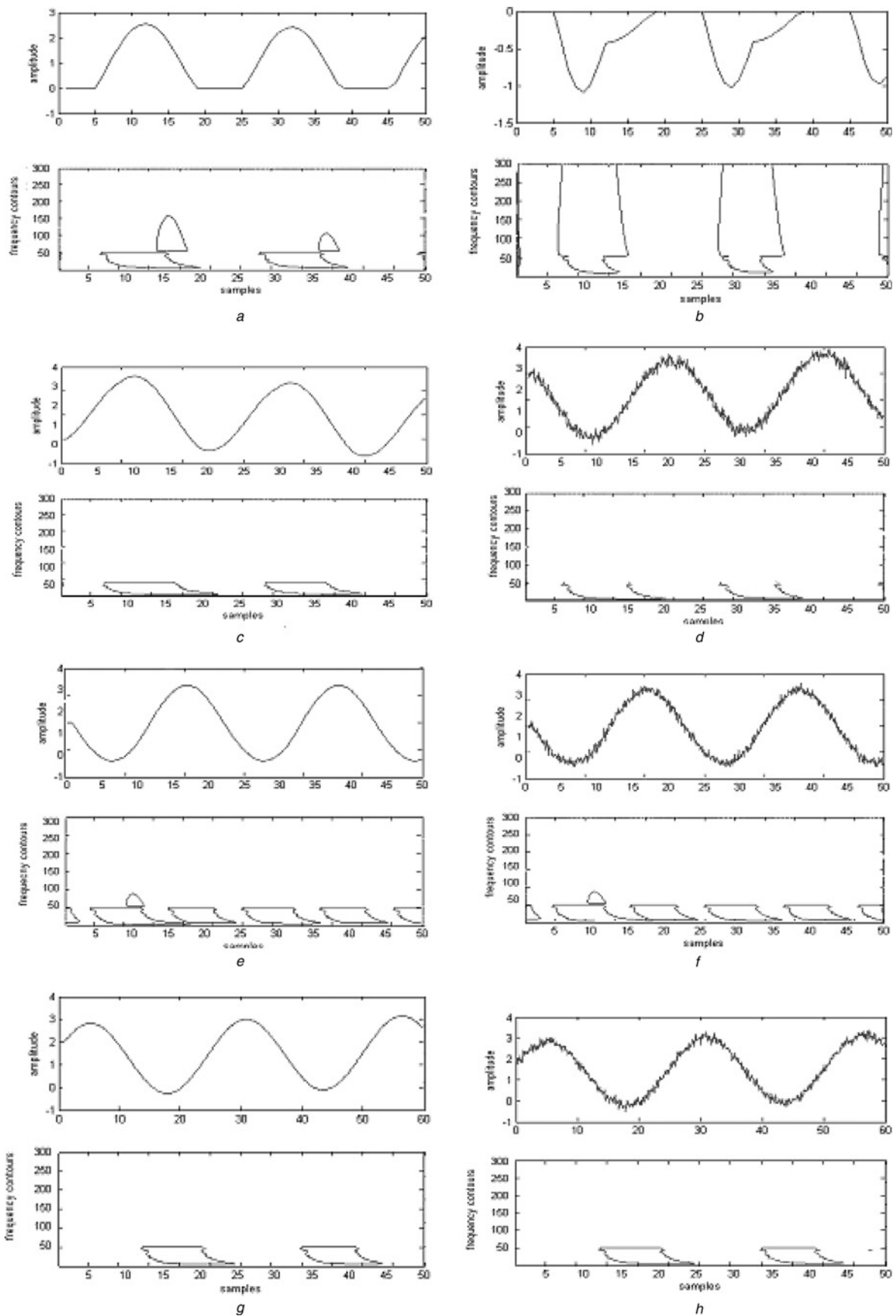


**Fig. 4** Frequency contours for simulation data at contour level-1 only

*a* S-contours for inrush current of a-phase at contour level 1

*b* S-contours for inrush current of b-phase at contour level 1

*c* S-contours for a-phase winding-winding fault (a-b fault) at contour level 1

*d* S-contours for b-phase winding-winding-ground fault (bc-g fault) at contour level-1 with SNR 20 dB

*e* S-contours for b-phase winding-winding fault (b-c fault) at contour level 1

*f* S-contours for inrush current of b-phase (b-c fault) at contour level 1 with SNR 20 dB

*g* S-contours for inrush current of c-phase (bc-g fault) at contour level 1

*h* S-contours for inrush current of c-phase (bc-g fault) at contour level 1 with SNR 20 dB

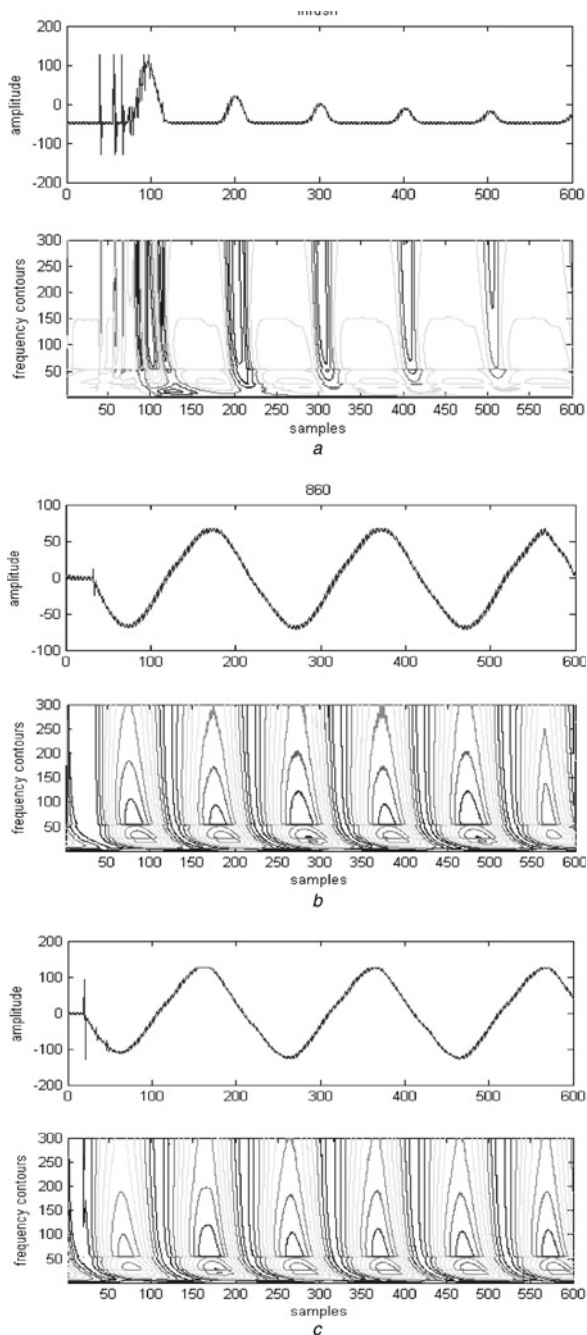


**Fig. 5** Frequency contours for real-time data  
*a* *S*-contours for inrush current (experimental data)  
*b* *S*-contours for 86–0% turn-to-turn fault (experimental data)  
*c* *S*-contours for 50–0% turn to turn faults (experimental data)

and 4.01 (minimum) and 5.48 (maximum) for internal faults for signals without noise. Also the energy index for signals with noise gives the similar result, which clearly distinguishes inrush from faults. Table 1 depicts the energy index for simulation test with 1000 MVA capacity and Table 2 provides the energy index for simulation test with 100 MVA capacity transformers. The energy index for the experimental set-up is given in Table 3. For experimental data, the energy index is above 1.65 for inrush current and 9.66 (maximum) and 6.07 (minimum) for internal faults, which clearly distinguishes faults from inrush condition.

To distinguish the inrush from internal faults, a suitable threshold value of 3.0 is set for energy index, below which it is inrush current and above which internal fault. The threshold value is chosen after testing the model under different operating conditions and capacities of the

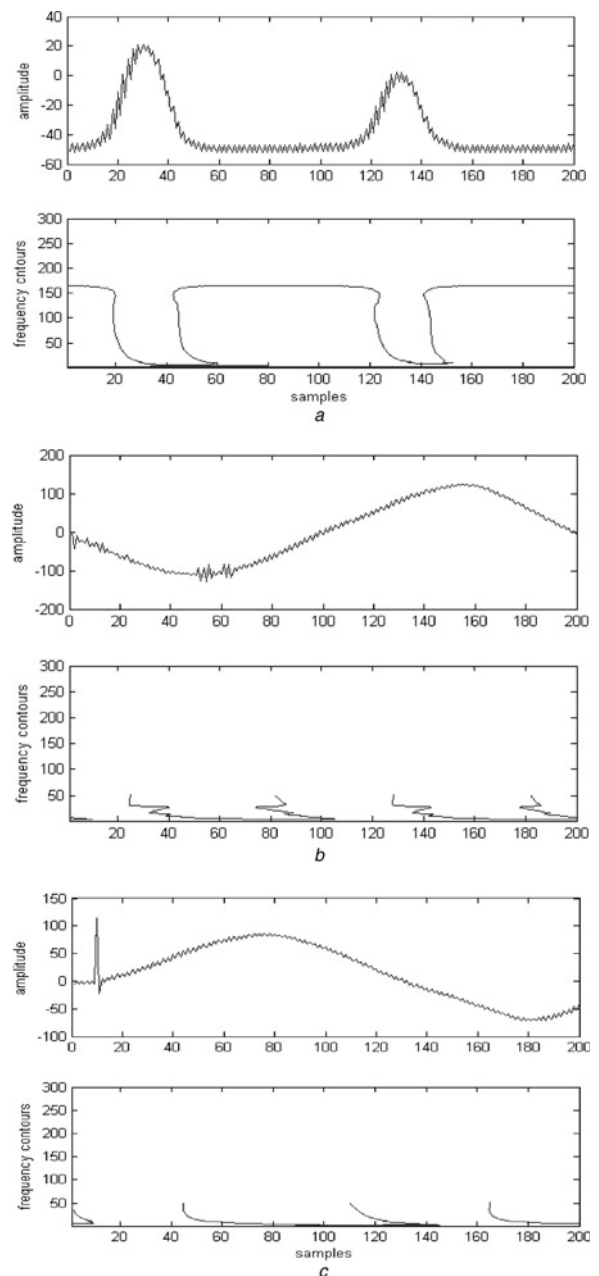


**Fig. 6** Frequency contours for real-time data at contour level-1 only

*a* *S*-contours for inrush current at contour level 1 (experimental data)  
*b* *S*-contours for inrush current at contour level 1 for 50-0 fault (experimental data)  
*c* *S*-contours for inrush current at contour level 1 for 50-86 fault (experimental data)

transformer. The tests have been done for 100 MVA and 1000 MVA transformers with different configuration such as Y-Y, Y-D, D-Y and D-D. It is found that the energy index is below 1.03 for inrush current and above 3.51 for internal faults taking both results into consideration for simulation study when the second harmonic magnitude compared with fundamental exceeds 20% and the fault current has a lower second harmonic component compared with the fundamental component.

As seen in Table 1, the proposed technique also works successfully where the second harmonic component is same (10–15%) in both inrush and internal faults. The energy index for 1000 MVA transformer is below 2.45 and above 3.24 for inrush and internal fault, respectively. Similarly, the energy indices for inrush and internal fault are 2.52 and 3.24, respectively, with SNR 20 dB. Also,

**Table 1: Energy and energy index for inrush and fault conditions for simulation data (1000 MVA transformers)**

Events (simulation data)	Energy (at contour level 1)	Energy (for contour levels 1–9)	Energy index	Energy (at contour level 1) (SNR 20 dB)	Energy (for contour levels 1–9 with SNR 20 dB)	Energy index (SNR 20 dB)
Inrush-a (Y-Y)	38.02	45.02	1.18	41.06	56.35	1.37
Inrush-b (Y-D)	32.64	35.64	1.09	39.64	45.23	1.14
Inrush-c (Y-Y)	36.78	40.12	1.09	34.65	42.65	1.23
Inrush-a (loaded) (D-D)	35.62	43.65	1.22	39.82	47.69	1.19
Inrush-b (loaded) (Y-Y)	29.64	33.54	1.13	35.48	39.48	1.11
Inrush-c (loaded) (Y-D)	32.87	36.98	1.12	32.98	37.45	1.13
a-g fault (Y-Y)	24.35	119.63	4.91	24.46	120.53	4.92
b-g fault (Y-D)	25.24	110.02	4.35	26.41	113.05	4.28
c-g fault (Y-Y)	24.15	114.32	4.73	24.58	104.03	4.23
a-b fault (a-phase) (D-Y)	21.97	120.53	5.48	22.23	153.06	6.88
a-b fault (b-phase) (D-D)	22.35	112.56	5.03	23.34	113.62	4.86
ca-g fault (a-phase) (D-Y)	24.52	115.64	4.71	24.76	110.25	4.45
ca-g fault (c-phase) (Y-Y)	21.26	120.65	5.67	21.34	114.68	5.37
bc-g fault (b-phase) (D-Y)	25.64	102.83	4.01	24.68	108.03	4.37
bc-g fault (c-phase) (D-D)	26.35	112.46	4.26	26.58	93.52	3.51
<b>Inrush and fault both contain 10–15% second harmonic</b>						
Inrush-a (Y-Y)	29.36	62.34	2.12	31.25	67.85	2.17
Inrush-b (Y-D)	31.26	60.57	1.93	32.65	61.58	1.88
Inrush-c (Y-Y)	29.64	72.68	2.45	30.68	77.59	2.52
a-b fault (a-phase) (D-Y)	25.63	88.96	3.47	26.31	94.85	3.60
a-b fault (b-phase) (D-D)	23.87	98.678	4.13	24.68	100.26	4.06
ca-g fault (a-phase) (D-Y)	22.68	73.68	3.24	23.68	76.84	3.24
ca-g fault (c-phase) (Y-Y)	21.48	82.68	3.84	22.64	86.35	3.81

**Table 2: Energy and energy index for inrush and fault conditions for simulation data (100 MVA transformers)**

Events (simulation data)	Energy (at contour level 1)	Energy (for contour levels 1–9)	Energy index	Energy (at contour level 1) (SNR 20 dB)	Energy (for contour level 1–9 with SNR 20 dB)	Energy index (SNR 20 dB)
Inrush-a (Y-Y)	36.25	41.65	1.14	38.91	55.12	1.41
Inrush-b (Y-D)	30.26	32.65	1.07	36.54	40.65	1.11
Inrush-c (Y-Y)	34.65	39.48	1.13	31.56	39.84	1.26
Inrush-a (loaded) (D-D)	32.65	40.21	1.23	36.58	42.78	1.16
Inrush-b (loaded) (Y-Y)	30.65	31.65	1.03	35.48	37.68	1.06
Inrush-c (loaded) (Y-D)	29.87	35.14	1.17	29.47	33.45	1.13
a-g fault (Y-Y)	22.65	111.65	4.92	22.64	112.65	4.97
b-g fault (Y-D)	21.65	120.65	5.57	23.54	111.62	4.74
c-g fault (Y-Y)	22.87	124.36	5.43	21.87	100.87	4.61
a-b fault (a-phase) (D-Y)	19.68	125.64	6.38	19.38	146.87	7.57
a-b fault (b-phase) (D-D)	20.46	109.64	5.35	21.56	109.84	5.09
ca-g fault (a-phase) (D-Y)	23.64	114.65	4.84	22.35	104.68	4.68
ca-g fault (c-phase) (Y-Y)	20.75	119.78	5.77	20.84	99.64	4.78
bc-g fault (b-phase) (D-Y)	22.65	120.65	5.32	23.48	102.47	4.36
bc-g fault (c-phase) (D-D)	23.48	118.65	5.05	25.57	101.58	3.97
<b>Inrush and fault both contain 10–15% second harmonic</b>						
Inrush-a (Y-Y)	29.68	66.54	2.24	31.25	66.54	2.12
Inrush-b (Y-D)	28.69	55.98	1.95	29.68	62.65	2.11
Inrush-c (Y-Y)	26.87	58.95	2.19	28.65	59.68	2.08
a-b fault (a-phase) (D-Y)	22.35	94.65	4.23	21.65	82.57	3.81
a-b fault (b-phase) (D-D)	24.68	88.21	3.57	25.14	81.69	3.24
ca-g fault (a-phase) (D-Y)	25.44	94.65	3.72	26.54	95.87	3.61
ca-g fault (c-phase) (Y-Y)	24.99	82.45	3.29	26.54	100.23	3.77

**Table 3: Energy and energy index for inrush and fault conditions for experimental data**

Events (experimental data)	Energy (at contour level 1)	Energy (for contour levels 1–9)	Energy index
Inrush (Y-Y)	91.56	142.65	1.55
Inrush (loaded)(Y-Y)	80.67	133.65	1.65
50-0 fault (Y-Y)	42.32	256.98	6.07
50-g fault (Y-Y)	33.68	325.64	9.66
86-0 fault (Y-Y)	46.87	314.85	6.71
86-g fault (Y-Y)	34.56	241.85	6.99
50-86 fault (Y-Y)	44.12	310.65	7.04
86-100 fault (Y-Y)	55.98	371.89	6.64
50-100 fault (Y-Y)	52.41	342.98	6.54

similar observations are made in Table 2 for 100 MVA transformers, where the energy index is below 2.24 and above 3.29 for inrush and internal fault, respectively. Similarly, the energy index is below 2.12 and above 3.24 for inrush and internal fault, respectively, with SNR 20 dB. The results for above cases are depicted in Tables 1 and 2 in bold and italics. The energy index is

1.65 for inrush and 6.07 for internal fault for experimental test as given in Table 3. Thus, from the above results, it is seen that the proposed technique works successfully where the second harmonic restraint fails. The flow chart to distinguish inrush current from fault is given in Fig. 7. In the proposed method, the energy content of *S*-transform of one cycle current signal is taken for calculation. The one cycle data takes 20 ms and time taken for *S*-transform and the algorithm is nearly 10 ms. Thus, the total time taken by the proposed protection scheme is 30 ms approximately from the inception of fault.

## 5 Conclusions

This paper presents a new approach for discrimination between inrush current and internal faults in power transformer by pattern recognition technique using *S*-transform. *S*-transform is found to be very powerful tool for non-stationary signal analysis and gives the frequency contours for inrush current and internal faults very distinctly as shown in the figures where second harmonic is pronounced in the case of inrush current compared with faults. The spectral energy is computed for inrush current and internal faults at different contour levels. The energy index is calculated to distinguish inrush current and internal faults. Also, the results under noisy conditions provide significant distinctions between faults and inrush. The proposed technique is compared with the existing differential protection based on second harmonic restraint and found successful compared to the later. Also the proposed one is very robust as *S*-transform is very less prone to noise compared with wavelet transform and so the application can be extended for protection schemes for large power transformers.

## 6 References

- Hon, S.N., and Qin, W.: 'A wavelet based method to discriminate between inrush and internal faults'. IEEE, 2000, pp. 927–931
- Youssef, O.A.S.: 'Discrimination between faults and magnetizing inrush currents in transformers based on wavelet transforms', *Electr. Power Syst. Res.*, 2002, **63**, pp. 87–94
- Pinnegar, C.R., and Mansinha, L.: 'Time local Fourier analysis with a scalable, phase modulated analyzing function: the *S*-transform with a complex window', *Signal Process.*, 2004, **84**, pp. 1167–1176
- Pinnegar, C.R., and Mansinha, L.: 'The *S*-transform with windows of arbitrary and varying window', *Geophysics*, 2003, **68**, pp. 381–385
- Mansinha, L., Stockwell, R.G., and Lowe, R.P.: 'Pattern analysis with two dimensional spectral localization: application of two-dimensional *S*-transforms', *Physica A*, 1997, **239**, pp. 286–295
- Liavanos, G., Ranganathan, N., and Jiang, J.: 'Heart sound analysis using the *S*-transform', *IEEE Comp. Cardiol.*, 2000, **27**, pp. 587–590
- Dash, P.K., Panigrahi, B.K., and Panda, G.: 'Power quality analysis using *S*-transform', *IEEE Trans. Power Deliv.*, 2003, **18**, (2), pp. 406–411
- Stockwell, R.G., Mansinha, L., and Lowe, R.P.: 'Localization of the complex spectrum: the *S*-transform', *IEEE Trans. Signal Process.*, 1996, **44**, pp. 998–1001
- Mao, P.L., and Aggarwal, R.K.: 'A novel approach to the classification of the transient phenomena in power transformers using combined wavelet transform and neural network', *IEEE Trans. Power Deliv.*, 2001, **16**, (4), pp. 654–660
- Jiang, F., Bo, Z.Q., Chin, P.S.M., Redfern, M.A., and Chen, Z.: 'Power transformer protection based on transient detection using discrete wavelet transform (DWT)'. IEEE, 2000
- Phadke, A.G., and Thorp, J.S.: 'Computer relay for power system' (Research Studies Press Ltd., 1998)
- Perez, L.G., Flechsig, A.J., Meador, J.L., and Obradovic, Z.: 'Training an artificial neural network to discriminate between magnetizing inrush and internal faults', *IEEE Trans. Power Deliv.*, 1994, **9**, (1), pp. 434–441
- Dash, P.K., Swain, D.P., Liew, A.C., and Rahman, S.: 'An adaptive linear combiner for on-line tracking of power system harmonics', *IEEE Trans Power Syst.*, 1996, **11**, (4), pp. 1730–1735

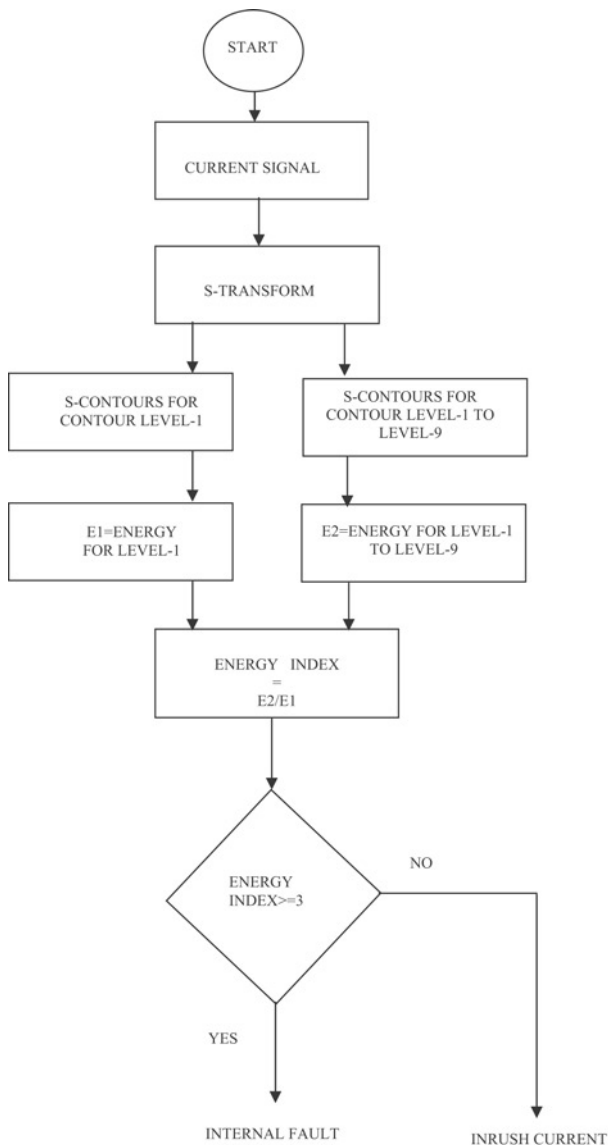


**Fig. 7** Flow chart to distinguish inrush current from internal faults